geoconvention
Calgary • Canada • May 7-11 2018

Q-Compensation by Iterative Time-Domain Deconvolution

Wubing Deng and Igor Morozov
University of Saskatchewan, wubing.deng@usask.ca, igor.morozov@usask.ca

Summary

Attenuation and dispersion effetcts in seismic wave propagation lead to reduced resolution and narrower bandwidths of seismic images. Traditional corrections for such effects, such as inverse-*Q* filtering, deconvolution, and spectral equalization focus on modifying the time-variant frequency-domain spectra of the records. Here, we propose a pure time-domain method offering significant advantages in the resolution and interpretational quality of the resulting images. Similar to wavelet transforms, the iterative time-domain deconvolution (ITD) represents the seismogram by a superposition of non-stationary source wavelets modelled in the appropriate attenuation model. Arbitrary frequency-dependent *Q* and velocity dispersion laws can be used, as well as non-*Q* type attenuation caused by focusing, defocusing, scattering, effects of fine layering, and fluctuations of the wavefield. We illustrate and compare the ITD to inverse-*Q* filtering by a realistic synthetic example. The example shows that the ITD is a practical and effective tool for *Q*-compensation with a broad scope of potential applications. An important benefit of ITD could be the ability to utilize geological information, such as locations and sparseness of major reflectors or presence of attenuation contrasts.

Introduction

Seismic waves are often affected by attenuation and dispersion caused by the inelasticity of the subsurface. In reflection seismic imaging, these effects are adverse and result in frequency-dependent reduction of amplitudes, narrowing down of the frequency bandwidths, and waveform phase distortions. Attenuation effects decrease the resolution of reflection seismic images, especially within deeper parts of the sections. Attenuation effects may also cause difficulties in imaging and interpretation, such as in horizontal event tracking and identification of small faults.

By studying the attenuation and dispersion in seismic records, two complementary objectives need to be recognized: 1) measuring these effects and including them in interpretation, and 2) removal of the adverse attenuation effects from final images. For the first objective, detailed knowledge of attenuation mechanisms is required. However, in most practical studies, detailed knowledge of the layering or rock-physics mechanisms of internal-friction is not available, and their determination is a subject of many studies. Nevertheless, even when the physical mechanisms are poorly known, attenuation and dispersion effects can be modelled empirically by constructing time-dependent attenuation operators. Generally, correction for these empirical operators represents some type of deconvolution (Hale, 1981) applied to the data.

In this paper, we propose using a time-domain method that is effective and offers several unique features for *Q* compensation. This time-domain method is a simple iterative algorithm popular in earthquake seismology (Kikuchi and Kanamori, 1982; Ligorría and Ammon, 1999), which we call the Iterative Time-domain Deconvolution (ITD) further in this paper. ITD represents the seismogram as a superposition of non-stationary source wavelets modelled by using an appropriate empirical attenuation model. Because of the use of an iterative data-fitting procedure in time domain, this approach can be viewed as a wavelet transform based on modelling the source waveform propagating through the section.

The time-domain formulation encourages application of numerous ideas beyond the traditional *Q*-compensation, such as combining multiple, true physical mechanisms of attenuation, scattering, or geometrical spreading (Morozov et al., in press), or deconvolution starting from stronger reflectors (as done by ITD). As a method using time-domain waveform matching, ITD can (in principle) incorporate additional information derived from geology, stacked seismic data or well logs, such as positions and sparseness of major reflectors or their sharp or gradational characters.

Theory

In time-variant deconvolution, a recorded seismic waveform can be regarded as a function $d(t, t_0)$ of two times defined at different scales: the two-way reflection time t_0 characterizing the depth of recording and the "local" wave time t near t_0. We implement this hierarchy of time scales by windowing the data using a sequence of overlapping time windows, as it is often done in time-variant filtering of seismic records (Yilmaz, 2001). Each windowed data (denoted $d(t,t_0)$) and reflectivity ($r(t,t_0)$) record is characterized by the time of its center t_0 and contains a Hanning taper applied to the respective continuous record. The tapered time windows are constructed so that the continuous reflectivity series represents a sum of windowed records: $r_{\text{complete}}(t) = \sum_{t_0} r(t, t_0)$, with analogous relations for data records $d_{\text{complete}}(t)$ before and after correction for attenuation.

The seismogram within a window centered at time t_0 can be represented by a convolution of the propagating seismic wavelet $w(t, t_0)$ and the reflectivity series $r(t,t_0)$:

$$d(t_0) = w(t_0) * r(t_0) \tag{1}$$

where dependences on t are implied in all factors, and symbol '$*$' denotes the convolution operation with respect to time t. For simplicity, we omit the additive noise in this convolutional model. Assume that the information about attenuation is not contained in $r(t_0)$ but in $w(t, t_0)$.

Let us now denote $w_{\text{el}}(t_0)$ an analogous "elastic" source waveform that would have been observed in the absence of attenuation. The corresponding seismic record $d_{\text{el}}(t_0)$ would be related to it by the same convolutional model:

$$d_{\text{el}}(t_0) = w_{\text{el}}(t_0) * r(t_0). \tag{2}$$

The actual $w(t_0)$ and $d(t_0)$ can then be related to $w_{\text{el}}(t_0)$ and $d_{\text{el}}(t_0)$ by a linear attenuation filter $a(t_0)$ (Hale, 1981):

$$w(t_0) = a(t_0) * w_{\text{el}}(t_0) \text{ and } d(t_0) = a(t_0) * d_{\text{el}}(t_0). \tag{3}$$

In this paper, we assume that w_{el} is known or can be estimated with satisfactory accuracy. The goal of attenuation compensation is to invert the second equation in (3) for the "elastic" data $d_{\text{el}}(t_0)$. This inversion is conventionally done in frequency domain, in which the local time t is replaced with angular frequency ω and the convolution becomes multiplication:

$$D(\omega, t_0) = A(\omega, t_0) D_{\text{el}}(\omega, t_0). \tag{4}$$

According to the usual convention, uppercase letters here represent Fourier transforms of the corresponding time-domain functions. The solution for obtaining the D_{el} is normally done by dividing both sides of eq. (4) by A with the application of some stabilization factor.

In order to obtain the ITD method, we propose a different approximate solution for D_{el} in eq. (4). Instead of solving the inverse problem for an operator A^{-1} in the frequency domain, let us perform the transformation $d(t_0) \to d_{\text{el}}(t_0)$ (or equivalently, $D(\omega, t_0) \to D_{\text{el}}(\omega, t_0)$) directly, by iteratively evaluating cross-correlations of the signal with the forward-modelled wavelet in the time domain. In the ITD method, the "reflectivity" series $r(t, t_0)$ within a window centered at t_0 is approximated by a series of pulses with amplitudes $r_i(t_0)$ located at times $\tau_i(t_0)$:

$$r(t, t_0) = \sum_{i=1}^{N} r_i(t_0) \delta(t - \tau_i(t_0)), \tag{5}$$

where $\delta(t)$ is the delta function. The number of pulses N per time window is either set by the analyst or selected adaptively based on waveform energy criteria described below. With few pulses, only the strongest reflections are reproduced, and with large N, the complete reflection series $r(t,t_0)$ is retained. By substituting eq. (5) into (1), the seismic record is presented by a superposition of wavelets of amplitudes r_i and placed at times τ_i:

$$d\left(t,t_0\right)=\sum_{i=1}^{N}r_i\left(t_0\right)w\left(t-\tau_i\left(t_0\right),t_0\right). \tag{6}$$

Instead of looking for a potentially unstable inverse of the wavelet, we solve equation (6) for the "reflectivity" series by using a synthetic wavelet $w(t_0)$ modelled at time t_0 by utilizing an appropriate combination of attenuation mechanisms. The search for $r_i(t_0)$ and $\tau_i(t_0)$ is iterative, starting from the largest value of $|r_1(t_0)|$ (Ligorría and Ammon, 1999). The corresponding time τ_1 is found by maximizing the cross-correlation between the data and the modelled (attenuated) source waveform: $\int d\left(t,t_0\right)w\left(t-\tau_1,t_0\right)dt$. The associated reflectivity amplitude r_1 is then given by the peak of cross-correlation:

$$r_1=\frac{\int d\left(t,t_0\right)w\left(t-\tau_1,t_0\right)dt}{\int w^2\left(t-\tau_1,t_0\right)dt}. \tag{7}$$

The rest of reflectivity parameters $r_i(t_0)$ and $\tau_i(t_0)$ are found by subtracting the prediction of the first peak from the waveform:

$$d\left(t,t_0\right)\rightarrow d_1\left(t,t_0\right)\equiv d\left(t,t_0\right)-r_1\,w\left(t-\tau_1,t_0\right) \tag{8}$$

repeating the same operations with $d_1(t,t_0)$ and continuing iteratively, with residual waveforms at n-th step defined by $d_n\left(t,t_0\right)\equiv d_{n-1}\left(t,t_0\right)-r_n\,w\left(t-\tau_n,t_0\right)$.

In the ITD procedure (7) and (8), the strongest contributions to the signal (6) are found first, and the iteration can be stopped based on several criteria. The simplest practical approach to stopping the iterations is to restrict the number of pulses N preprocessing window in the resulting solution (eq. (6)). The selection of N does not only help promoting the sparsity of the restored signal but also possesses the advantage of preferential recovery of the strongest reflections. The residual energy after n-th iteration is defined by

$$\varepsilon\left(n\right)\equiv\frac{\int d_n^2\left(t,t_0\right)dt}{\int d^2\left(t,t_0\right)dt}, \tag{9}$$

and can be used to evaluate what portion of the input signal is passed by the ITD filter. This parameter can also be used as a threshold for stopping the iterations.

After the resulting "sparse" "reflectivity" series $r(t_0)$ is determined, with convolve it with the "elastic" source waveform $w_{\mathrm{el}}\left(t_0\right)$, which gives the desired Q-compensated data record d_{el} as in eq. (2). Alternatively, instead of the source waveform, we can convolve $r(t_0)$ with a different shaping wavelet. In this case, the procedure would still perform Q-compensation (because of eliminating the modeled effect of attenuation and dispersion), but it would also contain spectral- and phase-correction properties of deconvolution.

The key advantages of the ITD (and similar time-domain) procedure are the absence of inverse operator A^{-1} and therefore stability and absence of spectral regularization parameters. In addition, the underlying "reflection" sequence $r(t_0)$ that can be analyzed and potentially interpreted, which may provide additional outcomes and constraints on the procedure.

Examples

To illustrate the performance of the ITD algorithm on a realistic reflection waveform, we show here a single 1200 ms-long trace selected from post-stack Marmousi-II synthetics modelled with attenuation quality factor $Q = \infty$, 10, and 50 (Figure 1). The synthetics were modelled by using vertical wave propagation, the convolutional model, and only considering the primary reflections. The noise level in this example is low (as resulting from numerical synthetics), and here we are only interested in the recovery of complex reflection waveforms. Both modelling and ITD were performed by using a 30-Hz Ricker wavelet. To perform the post-stack ITD iterations, we selected 200-ms time windows, threshold parameter $N = 200$, and the residual energy $\varepsilon = 10^{-7}$. In the inverse-*Q* algorithm, the stabilization factor was set equal 0.005.

For $Q = 50$ (Figure 1b), comparisons of the filtered records (black lines) to the record modelled in an elastic model (grey lines) show that ITD accurately recovers practically the complete elastic record (Figures 1b). For very strong attenuation ($Q = 10$; Figure 1a), ITD recovers well the reflections above about 700 ms and the stronger reflections from the deeper part of the trace (for example, near times equal 1050, 1150, and 1450 ms) (Figure 1a).

Compared to the inverse-*Q* filtering, ITD results appear to be preferable in both cases (Figures 1a and b). For $Q = 50$, the quality of inverse-*Q* correction is good above about 800 ms and reduces with depth (Figure 1b). The strong reflection packages near 850–900 ms and 1400 ms are somewhat under-corrected in amplitudes and shifted in phases. For very strong attenuation, the inverse-*Q* filtering result appears unsuccessful (Figure 1a). These difficulties in inverse-*Q* filtering are apparently caused by the selections of the stabilization factor required for suppressing the high-frequency noise in these records. In this low-noise example, this stabilization factor or gain limiting could of course be adjusted and results comparable to those of ITD achieved. However, our goal in this example was to illustrate the inverse-*Q* and ITD filtering with “typical” parameters not tailored for a noise-free case.

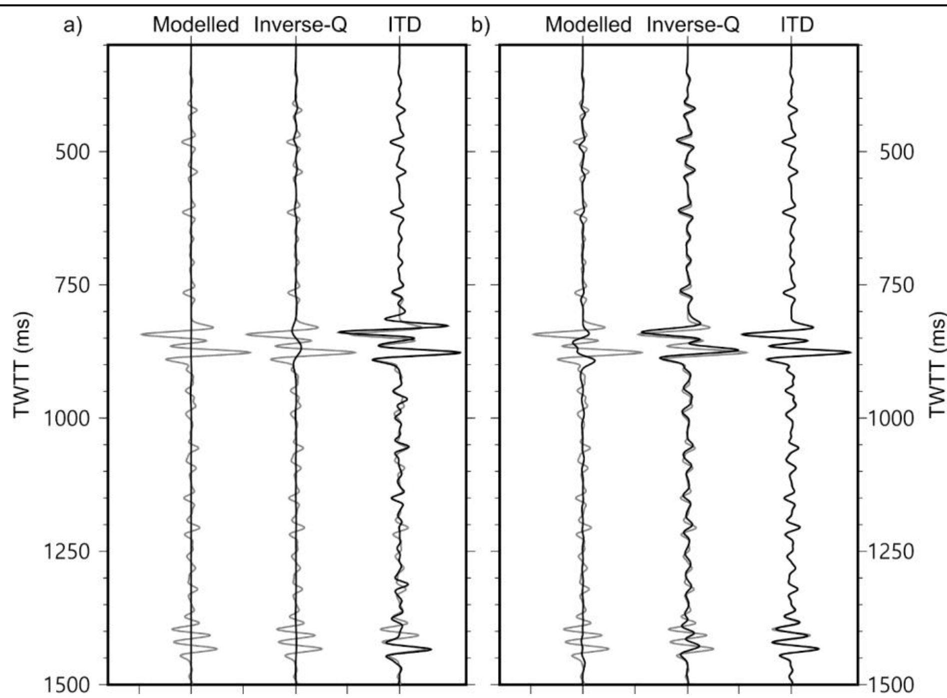

Figure 1. Comparisons between the attenuated reflection records modelled in Marmousi-II model, its inverse-*Q* filtered record and ITD-corrected records (black lines, labels). Panels a) and b) correspond to modelled levels of $Q = 10$ and 50, respectively. The identical grey lines in all plots are the models in an elastic structure ($Q = \infty$). All records are scaled equally, and therefore the attenuated records (labels “Modelled”) show low amplitudes in these plots, particularly in plot a).

Thus, the presented simple but detailed example shows that ITD performs successfully in cases where the conventional inverse-*Q* filtering works, but the ITD can also be effective and more accurate in cases difficult for inverse-*Q* filtering. Real-data examples showing significant additional image enhancements by ITD are shown by Morozov et al. (in press). As shown by our ongoing research, the ITD is also relatively stable with respect to additive random noise, uncertainties in the measurements of *Q* and in the selection of the source wavelet.

Conclusions

We present a case for a broad class of time-variant, time-domain deconvolution methods for *Q*-compensation of reflection seismic records. In particular, a simple scheme called the iterative time-domain deconvolution (ITD) appears to offer a number of unique advantages. ITD is performed on a trace-by-trace basis, and consequently it can be used in both post- and pre-stack processing and potentially included in migration. The performance of the method was illustrated by using a realistic synthetic example.

Acknowledgements

Figure 1 was produced by using Generic Mapping Tools (http://gmt.soest.hawaii.edu/).

References

Hale D. 1981. An inverse Q-filter. Stanford Exploration Project 26, 231−244.

Kikuchi M. and Kanamori H. 1982. Inversion of complex body waves. Bulletin of the Seismological Society of America 72, 491−506.

Ligorría J. P. and Ammon C. J. 1999. Iterative deconvolution and receiver-function estimation. Bulletin of the Seismological Society of America 89, 1395−1400.

Morozov, I. B., M. Haiba., and W. Deng, Inverse attenuation-filtering, Geophysics, in press.

van der Baan M. 2012. Bandwidth enhancement: Inverse Q filtering or time-varying Wiener deconvolution?. Geophysics 77, (4), V133−V142.

Wang Y. 2008. Seismic inverse Q filtering. Blackwell. ISBN 978-1-4051-8540-0.

Yilmaz O. 2001. Seismic data processing Society of Exploration Geophysicists. ISBN 978-1-56080-094-1